ANALYSIS OF SOLAR HEATING OF A SNOWPACK

Leonid A. Dombrovsky and Alexander A. Kokhanovsky

Following from: *Computational models for combined heat transfer in snow and ice*

Consider first a model problem to understand the main special features of solar radiation transfer in a snowpack. Obviously, a contribution of the direct solar radiation to the snowpack heating is predominant as compared with the sky radiation. Therefore, it is sufficient to consider the absorbed power of solar radiation at various values of zenith angle θ_{sol}. It is assumed that the spectrum of the incident solar radiation is similar to the blackbody radiation at temperature $T_{\text{sol}} = 6000\text{K}$. The calculated relative values of the integral radiation power, $\bar{P}_{\text{t}} = \int_0^\infty P(z)\,\mathrm{d}z / \int_{\lambda_{\min}}^{\lambda_{\max}} I_{\text{b}}(T_{\text{sol}}, \lambda)\,\mathrm{d}\lambda$ (I_{b} is the Planck function), absorbed in a snowpack containing ice grains of different size are presented in Fig. 1. It is known that the spectrum of solar radiation is quite different at large zenith angles. Therefore, this range of θ_{sol} is not shown in Fig. 1.

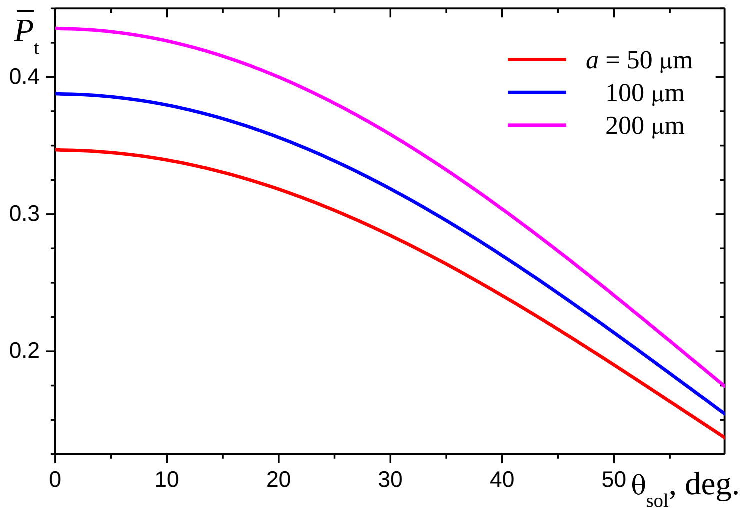

Figure 1. The normalized radiative power absorbed in an optically thick snowpack.

As one can expect, the main part of solar radiation is reflected from the snowpack because of a strong reflection of the visible radiation. One can see that $\bar{P}_{\text{t}}$ decreases considerably with the zenith angle, whereas the effect of ice grain size is insignificant. It should be also recalled that the calculations by Dombrovsky et al. (2019) for polydisperse spherical ice grains showed that one can use the monodisperse approximation with an equivalent mean radius of the grains to obtain the spectral properties of snow.

The depth of the radiation propagation into the snowpack is illustrated in Fig. 2 by calculations at normal incidence. The contributions of the visible range ($\lambda < 0.78\mu\text{m}$) and the near-infrared range to the absorbed radiation power are calculated separately:

$$\bar{P}(z) = \bar{P}_{\text{vis}}(z) + \bar{P}_{\text{ni}}(z) \qquad \{\bar{P}_{\text{vis}}, \bar{P}_{\text{ni}}\} = \{P_{\text{vis}}, P_{\text{ni}}\} / \int_{\lambda_{\min}}^{\lambda_{\max}} I_b(T_{\text{sol}}, \lambda)\, \mathrm{d}\lambda \tag{1}$$

The universal coordinates $f_v z$ and $\bar{P}/f_v$ are used in Fig. 2 to present the results for various values of f_{v} (the ratio of snow density to ice density). At realistic value of $f_{\text{v}} = 0.33$, the near-infrared radiation is absorbed mainly in a thin surface layer of snowpack, whereas the visible radiation is absorbed almost uniformly in the layer of thickness about 60 mm and its contribution to heating deep layers of snowpack is expected to be considerable. This result agrees well with the conclusion by Munneke et al. (2009) about an important role of the deep penetration of short-wave solar radiation in the heat balance of a snowpack. The effect of grain size on this effect is not strong. Therefore, the subsequent calculations are performed at $a = 100\mu\text{m}$.

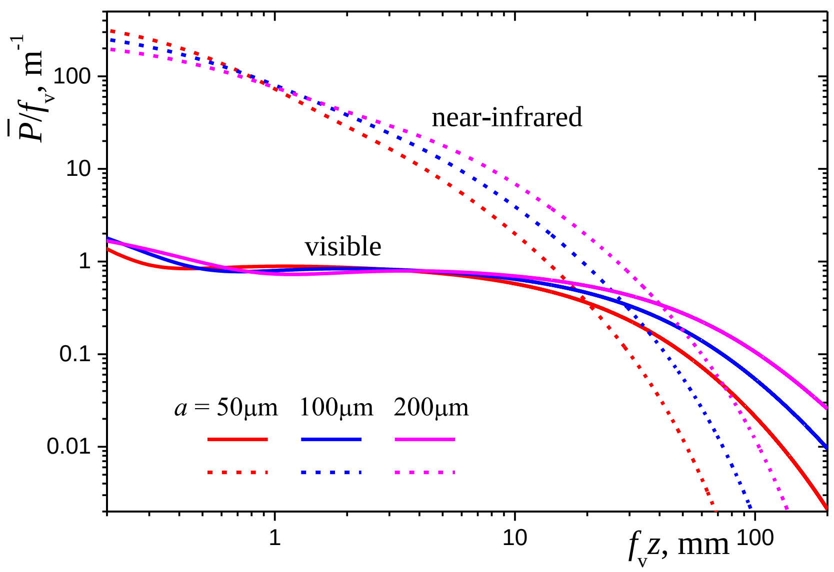

Figure 2. Contributions of the visible range ($\bar{P}_{\text{vis}}$) and near-infrared range ($\bar{P}_{\text{ni}}$) to the profiles of normalized absorbed radiation power in a snowpack.

It is interesting to analyze the results obtained at realistic parameters of the problem. The range of snow density variation from $\rho = 100\text{kg/m}^3$ to 550 kg/m^3 leads to the corresponding variations in thermal properties of snow. Obviously, the volumetric heat capacity, ρc, is directly proportional to the density, whereas the thermal conductivity of snow exhibits more strong increase with the snow density. In addition, at the same snow density, variations in snow microstructure can change thermal conductivity by a factor of two. Thermal conductivity of snow has been studied in many papers. Most of the results obtained are discussed in a review paper by Arenson et al. (2015). It was shown that thermal conductivity is almost directly proportional to the square of density and varies from $k = 0.04\text{W/(m K)}$ to 1W/(m K). The temperature variations of thermal properties of snow are relatively small and the effect of temperature on snow density and thermal properties is not considered. The constant values of $k = 0.2\text{W/(m K)}$ and $\rho c = 0.6\text{MJ/(m}^3\text{K)}$ corresponding to the volume fraction of ice grains of $f_{\text{v}} = 0.33$ are used in the calculations.

In the midsummer (summer solstice), the current declination of the Sun is equal to $\delta = 23.44^{\circ}$. This value of δ is used to determine the solar zenith angle:

$$\cos\theta_{\mathrm{sol}} = \sin\phi\,\sin\delta + \cos\phi\,\cos\delta\,\cos\chi \qquad (2)$$

where ϕ is the local latitude and χ is the hour angle. The value of $\phi = 70^{\circ}$ is considered in the calculations. The following relation is used to determine the value of χ for the current time, t, measured in hours from the midnight:

$$\chi = \pi|1 - t_1/12| \qquad t_1 = t - 24\lfloor t/24 \rfloor \qquad (3)$$

where symbol $\lfloor\ \rfloor$ denotes the floor function. The resulting variation of θ_{sol} with the local solar time is shown in Fig. 3. The effect of a sloping surface of snow is also considered below. There are many possible orientations of the sloping surface with respect to the visible path of the Sun. The simplest orientation can be treated as a variation of the declination angle. Time variation of the solar zenith angle for such a surface with a sloping angle $\vartheta_{\mathrm{sl}} = 10^{\circ}$ is also shown in Fig. 3.

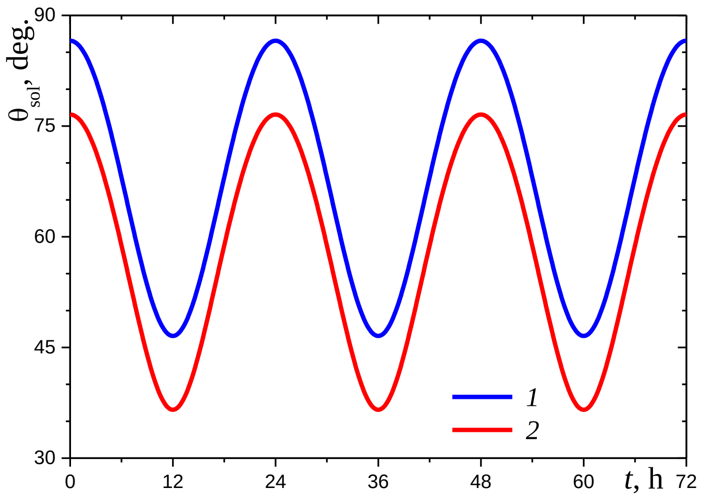

Figure 3. Time variation of solar zenith angle considered in the case problem: *1* – horizontal surface, *2* – sloping surface at $\vartheta_{\mathrm{sl}} = 10^{\circ}$.

The spectral radiative flux from the Sun and clear sky to the horizontal earth surface are presented in Fig. 4. The spectral dependencies were calculated using the SBDART code (Ricchiazzi et al. 1998). The choice of solar zenith angles is determined by the case problem parameters. Generally speaking, the contribution of direct solar radiation is much greater than that of diffuse radiation from the sky. However, it is not the case for visible light at solar zenith angles $\theta_{\mathrm{sol}} > 60^{\circ}$. Therefore, the sky radiation is taken into account in the calculations.

According to (Dombrovsky et al. 2019), the following analytical expressions for the everyday variation of coefficients of convective heat transfer and radiative cooling are considered:

$$h = h_{\min} + (h_{\max} - h_{\min})\psi(\theta_{\mathrm{sol}}) \qquad \varepsilon = 1 - F(\theta_{\mathrm{sol}}) \qquad (4a)$$

$$\psi(\theta_{\mathrm{sol}}) = \begin{cases} 1, & 0 \le \theta_{\mathrm{sol}} < 4\pi/9 \\ 0.5 - 0.5\sin(18\theta_{\mathrm{sol}} - 8.5\pi), & 4\pi/9 \le \theta_{\mathrm{sol}} < \pi/2 \end{cases} \qquad (4b)$$

It is assumed in Eqs. (4a) and (4b) that the midnight conditions approach gradually starting from $\theta_{\mathrm{sol}} = 80^o$. Note that the values of $h_{\mathrm{max}} = 10$ W/(m^2 K) and 15 W/(m^2 K) correspond to a weak wind (with a speed less that about 1–2 m/s) and to a moderate wind of speed about 3 m/s, respectively (Defraeye et al. 2011, Mirsadeghi et al. 2013), whereas $h_{\mathrm{min}} = 6$ W/(m^2 K) is used for ~~the~~ windless weather.

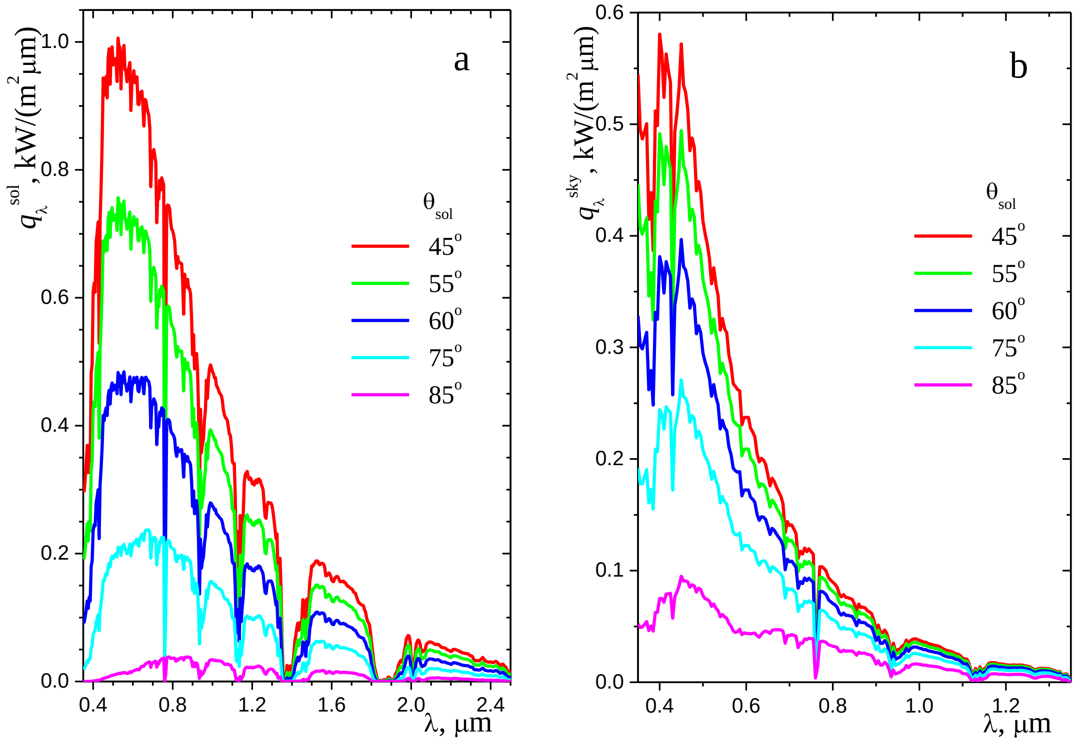

Figure 4. The spectral radiative flux at the earth surface:

a – direct radiation from the Sun, b – diffuse radiation from the clear sky.

The temperature profiles in a snowpack calculated for the first day at $T_0 = T_{\mathrm{air}}(z) = -10^{\circ}$C are presented in Fig. 5. One can see that the snowpack is heated rather fast in the morning and the melting temperature is reached at noon. A further evolution of the snowpack temperature depends strongly on wind speed. In the afternoon, the maximum temperature of snow is predicted at the distance about 15 mm from the snow surface at 6 pm and h_{max}=15 W/(m^2 K). The evening and night cooling of snowpack takes place for the surface layer of thickness from 15 mm to about 120 mm, whereas a continuous heat conduction leads to further heating of deep layers of the snowpack.

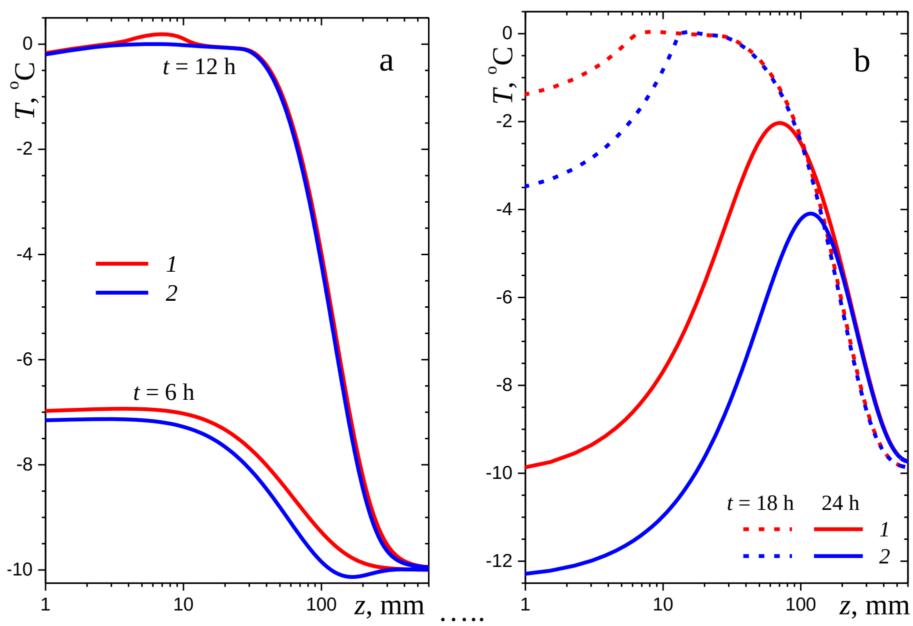

Figure 5. Typical profiles of temperature in snowpack (a) before the noon and (b) after the noon: *1* – h_{max} = 10 W/(m^2 K), *2* – 15 W/(m^2 K).

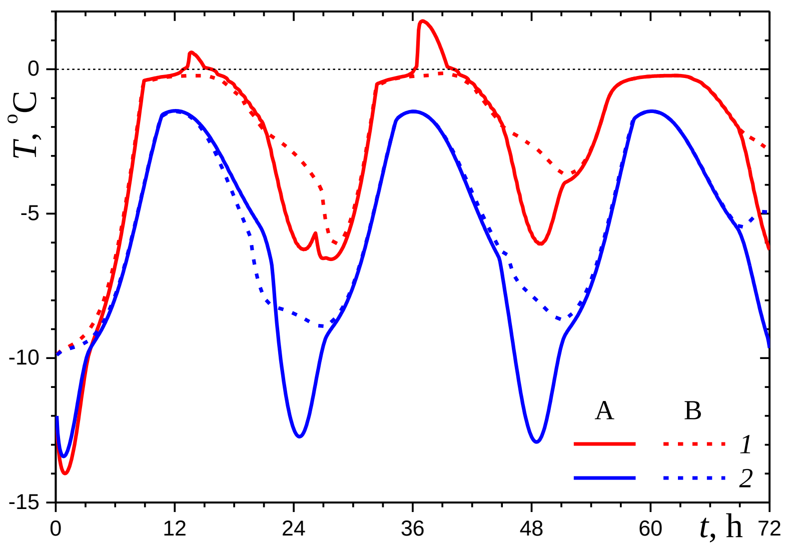

Figure 6. The effect of wind on snow surface temperature: *1* – h_{max} = 8 W/(m^2 K) (weak wind), *2* – 15 W/(m^2 K) (moderate wind); A – complete calculation, B – without radiative cooling.

The computational results for the three-day variation of snow surface temperature presented in Fig. 6 show an almost periodic variation of the temperature with a great difference between the day and the night. The effects of both the convective heat transfer in windy weather and the radiative cooling of a snowpack surface are significant. It is interesting that radiative cooling is partially compensated by a relatively long convective heating. The latter may lead to the unexpectedly strong surface heating and even melting as compared with the computational predictions ignoring the radiative cooling. This physical result of combined transient heat transfer in a snowpack was obtained by Dombrovsky et al. (2019) for the first time. Note that the details of temperature behavior near the melting temperature are explained by the finite value of $\Delta T = 0.1$K used in the calculations.

Similar calculations for the better irradiated sloping surface of snowpack with $\vartheta_{sl} = 10^{o}$ can be easily calculated by multiplying the directional radiative flux at solar zenith angle $\theta_{sol}(t)$ by the ratio of $cos(\theta_{sol}^{sl})/\cos(\theta_{sol})$. Note that the conventional night-time conditions including the radiative cooling do not take place for the sloping surface considered. The overall effect of snow surface sloping on time variation of snowpack surface temperature is shown in Fig. 7. Obviously, the snow surface turned to the Sun exhibits a higher temperature, especially in the time of large zenith angle of the Sun. It means that specific conditions of solar irradiation cannot be ignored even at sloping angle of $\vartheta_{sl} = 10^{o}$.

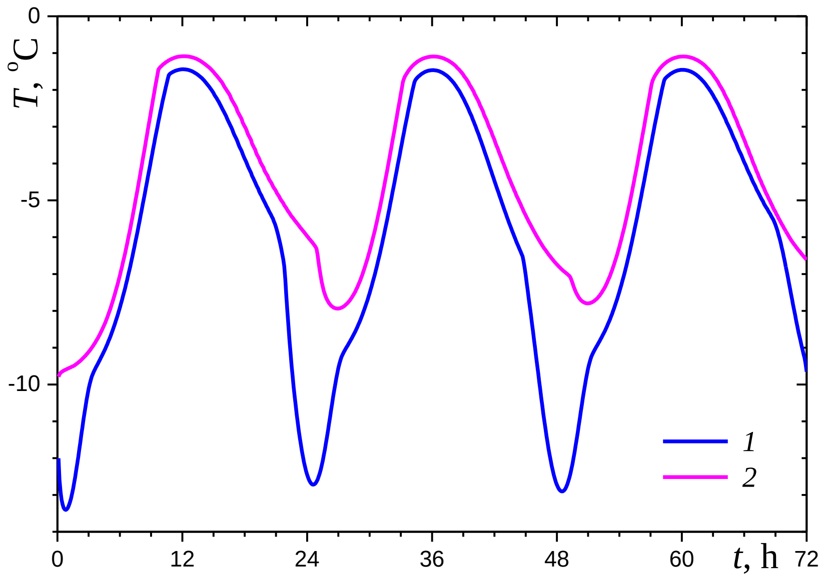

Figure 7. Effect of sloping of snowpack surface on the time variation of surface temperature: *1* – horizontal surface, *2* – sloping surface ($\vartheta_{sl} = 10^{o}$). Calculations at $h_{max} = 15$ W/(m^2 K).

The results obtained make clear a contribution of the visible and near-infrared solar radiation as well as the role of convective cooling or heating of snow, mid-infrared radiative cooling of snow surface, and continuous heating of deep snow layers due to heat conduction. The numerical analysis indicates a deep heating of snowpack and relatively strong effect of wind and radiative cooling on surface temperature of snow. The calculations for the case problem demonstrated the main possibilities of the computational model, which is expected to be a convenient and useful tool in further studies of snowpack solar heating.

References

Arenson, L.U., Colgan, W., and Marshall, H.P. (2015) Physical, Thermal, and Mechanical Properties of Snow, Ice, and Permafrost, Chapter 2 in "*Snow and Ice-Related Hazards, Risk and Disasters*", 35-75.

Defraeye, T., Blocken, B., and Carmeliet, J. (2011) Convective Heat Transfer for Exterior Building Surfaces: Existing Correlations and CFD Modelling, *Energy Convers. Manag.*, 52 (1): 512-522.

Dombrovsky, L.A., Kokhanovsky, A.A., and Randrianalisoa, J.H. (2019) On Snowpack Heating by Solar Radiation: A Computational Model, *J. Quant. Spectrosc. Radiat. Transf.*, 227: 72-85.

Mirsadeghi, M., Cóstola, D., Blocken, B., and Hensen, J.L.M. (2013) Review of External Convective Heat Transfer Coefficient Models in Building Energy Simulation Programs: Implementation and Uncertainty, *Appl. Therm. Eng.*, 56 (1-2): 134-151.

Munneke, P.K., van den Broeke, M.R., Reijmer, C.H., Helsen, M.M., Boot, W., Schneebeli, M, and Steffen, K. (2009) The Role of Radiation Penetration in the Energy Budget of the Snowpack at Summit, Greenland, *The Cryosphere*, 3 (2): 155-165.

Ricchiazzi, P., Yang, S., Gautier, C., and Sowle, D. (1998) SBDART: A Research and Teaching Software for Plane-Parallel Radiative Transfer in the Earth Atmosphere, *Bull. Am. Meteorol. Soc.*, 79 (10): 2101-2114.